NeuroImage: Clinical 22 (2019) 101739

Contents lists available at ScienceDirect

NeuroImage: Clinical

journal homepage: www.elsevier.com/locate/ynicl

A multicenter study of ketamine effects on functional connectivity: Large scale network relationships, hubs and symptom mechanisms

Leah M. Fleming[a,b], Daniel C. Javitt[c,d], Cameron S. Carter[e], Joshua T. Kantrowitz[c,d], Ragy R. Girgis[c], Lawrence S. Kegeles[c], John D. Ragland[e], Richard J. Maddock[e], Tyler A. Lesh[e], Costin Tanase[e], James Robinson[d], William Z. Potter[f], Marlene Carlson[c], Melanie M. Wall[c,f], Tse-Hwei Choo[c], Jack Grinband[c], Jeffrey Lieberman[c], John H. Krystal[a,1], Philip R. Corlett[a,*,1]

[a] Department of Psychiatry, Yale University, New Haven, CT, United States of America
[b] Interdepartmental Neuroscience Program, Yale University, New Haven, CT, United States of America
[c] Department of Psychiatry, New York State Psychiatric Institute, Columbia University Medical Center, New York, NY, United States of America
[d] Nathan Kline Institute for Psychiatric Research, Orangeburg, New York, NY, United States of America
[e] Department of Psychiatry, University of California, Davis, United States of America
[f] National Institute of Mental Health, Rockville, MD, United States of America

ARTICLE INFO

Keywords:
Ketamine
Functional connectivity
Psychosis
Resting state

ABSTRACT

Ketamine is an uncompetitive *N*-methyl-D-aspartate (NMDA) glutamate receptor antagonist. It induces effects in healthy individuals that mimic symptoms associated with schizophrenia. We sought to root these experiences in altered brain function, specifically aberrant resting state functional connectivity (rsfMRI). In the present study, we acquired rsfMRI data under ketamine and placebo in a between-subjects design and analyzed seed-based measures of rsfMRI using large-scale networks, dorsolateral prefrontal cortex (DLPFC) and sub-nuclei of the thalamus. We found ketamine-induced alterations in rsfMRI connectivity similar to those seen in patients with schizophrenia, some changes that may be more comparable to early stages of schizophrenia, and other connectivity signatures seen in patients that ketamine did not recreate. We do not find any circuits from our regions of interest that correlates with positive symptoms of schizophrenia in our sample, although we find that DLPFC connectivity with ACC does correlate with a mood measure. These results provide support for ketamine's use as a model of certain biomarkers of schizophrenia, particularly for early or at-risk patients.

1. Introduction

Ketamine is an uncompetitive *N*-methyl-D-aspartate (NMDA) receptor antagonist used in healthy volunteers as a safe, transient model of the symptoms of schizophrenia (Krystal et al., 1994; Krystal et al., 2003). Ketamine induces delusion-like ideas, thought disorder, tangential speech, negative symptoms, working memory (WM) deficits, and illusory percepts (Corlett et al., 2007a; Driesen et al., 2013a; Anticevic and Corlett, 2012). Similarities between the neural effects of ketamine and findings in schizophrenia (reviewed in: Haaf et al., 2018 & Frohlich and Van Horn, 2013) have also supported ketamine's use in modeling these symptoms (Krystal et al., 2003; Krystal et al., 2017). This work has implicated perturbed NMDA receptor function and glutamate transmission in the pathophysiology of schizophrenia (Balu, 2016). Interestingly, ketamine has also been shown to have affects on mood symptoms and act as a rapid-acting antidepressant, which is not relevant to its use as a model of schizophrenia but could be relevant to some of the changes in brain connectivity previous reported under ketamine.

There is a vastly expanding literature on changes in functional connectivity (fc) observed in patients with schizophrenia, particularly during resting state (Driesen et al., 2013b; Anticevic et al., 2014a;

Abbreviations: DMN, default mode network; FPN, frontoparietal network; DAN, dorsal attention network; SAL, salience network; DLPFC, dorsolateral prefrontal cortex; MD, mediodorsal; LGN, lateral geniculate nucleus; ACC, amterior cingulate cortex; PCC, posterior cingulate cortex; BPRS, Brief Psychaitry Rating Scale; CADSS, Clinician Administered Dissociative Symptom Scale; POMS, Profile of Mood States; mPFC, medial prefrontal cortex; IPL, Inferior Parietal Lobe; IPS, intraparietal sulcus; pIPS, posterior IPS; aIPS, anterior IPS; FEF, frontal eye field; PPC, posterior parietal cortex

* Corresponding author at: Connecticut Mental Health Center, 34 Park Street, New Haven, CT 06511, United States of America.
E-mail address: philip.corlett@yale.edu (P.R. Corlett).

[1] These authors contributed equally.

https://doi.org/10.1016/j.nicl.2019.101739
Received 25 September 2018; Received in revised form 24 February 2019; Accepted 27 February 2019
Available online 28 February 2019

Anticevic et al., 2014b; Lefort-Besnard et al., 2018; Zhou et al., 2017). It would be useful to determine which biomarkers associated with schizophrenia are also present following ketamine infusions, and whether these correlate with various psychotic symptoms specifically. This is important for making inferences about the relationships between NMDA dysfunction, fc changes, and symptoms of schizophrenia. We assessed changes in fc in participants given relatively high doses of ketamine compared to saline infusion during rest. We focused on those changes highlighted by meta-analyses of resting fc in schizophrenia (Sheffield and Barch, 2016; Li et al., 2017) that have a relationship with psychotic symptoms in patients (Whitfield-Gabrieli et al., 2009; Zhou et al., 2017; Ferri et al., 2018). Others have recently studied the effects of ketamine on connectivity with some of these regions at sub-anesthetic (Mueller et al., 2018) and various anesthetic (Bonhomme et al., 2016) doses. However, we were particularly interested in the relationships of these functional connectivity changes with psychotic symptoms, so we used higher sub-anasthetic doses of ketamine and a greater number of participants administered ketamine in order to assess these symptom correlations.

First, we assayed fc of the default-mode network (DMN), particularly with regions within "task-positive networks" including the dorsal attention network (DAN) and fronto-parietal control network (FPN). The default mode network is generally more active during "rest" scans or social cognition tasks, whereas these task positive networks (TPN) are generally more active during tasks such as those involving working memory than rest (reviewed in Raichle, 2015). Therefore these networks have an anti-correlated relationship with each other. A decrease in this standard anti-correlation between the DMN and the FPN has been observed in patients with schizophrenia during both rest and a WM task, and this correlated with WM performance and positive symptoms (Whitfield-Gabrieli et al., 2009). This has also been shown in participants given ketamine during a WM task (Anticevic et al., 2012). Similarly, disruptions in fc between the DMN and DAN have been observed in patients with schizophrenia during rest (Lefort-Besnard et al., 2018) and during a WM task (Zhou et al., 2017), although the directions of change varied across sub-regions of these networks at rest (Lefort-Besnard et al., 2018). We conducted seed-based analyses using the average time series of all of the combined regions within each of these networks in order to determine whether large-scale network dynamics were altered by ketamine at rest. Unlike previous work using a representative seed within each network (Mueller et al., 2018), we wanted to explore the interactions between these networks as a whole. Our results also led us to follow up with a specific analysis of the differences in connectivity, under ketamine versus saline, between the "salience network" (SAL) and the DAN, FPN and DMN. The salience network has been shown to mediate the anti-correlation between task positive networks and the DMN (Chen et al., 2013; Zhou et al., 2018).

Next, we assessed the effects of ketamine on connectivity between the right DLPFC and other voxels in the brain compared to saline. The DLPFC is a region within the FPN that has consistently been implicated in working memory deficits in schizophrenia (Anticevic and Corlett, 2012; Driesen et al., 2013b; Corlett et al., 2006; Whitfield-Gabrieli et al., 2009), as well as prediction error deficits and delusions in psychosis for the right DLPFC specifically (Corlett et al., 2006; Corlett et al., 2007b). Similarly, participants given ketamine show working memory deficits and coinciding alterations in DLPFC connectivity during WM tasks (Driesen et al., 2013a). NMDA dysfunction may therefore play a role in the DLPFC dysconnectivity and WM impairment in schizophrenia. Additionally, in patients with schizophrenia, the strongest shift in the anti-correlation of task positive regions with seeds of the DMN has been observed in the right DLPFC during rest (Whitfield-Gabrieli et al., 2009). This has inspired others to explore alterations in DLPFC fc under ketamine during rest as a representation of task-positive network connectivity changes (Mueller et al., 2018). Our combination of the FPN network and a more targeted right DLPFC-based analysis could identify region-specific trends in addition to the large-scale network dynamics under ketamine during rest in the same group of participants.

We also examined the effect of ketamine versus saline on connectivity between two nuclei within the thalamus and the rest of the brain. In patients with schizophrenia, alterations in the connectivity between the thalamus and sensory-motor cortices, as well as prefrontal, striatal and cerebellar regions have been reported (Anticevic et al., 2014a; Li et al., 2017; Ferri et al., 2018), and shown to correlate with positive symptoms (Ferri et al., 2018). These effects were shown to be localized to two nuclei of the thalamus that are heavily connected with the PFC and primary visual cortex: the medio-dorsal (MD) nucleus and lateral geniculate nucleus (LGN) (Anticevic et al., 2014a). Using the MD nucleus and the LGN as seeds, Anticevic et al. (2014a) showed that both of these nuclei have uniquely altered connectivity patterns in patients with schizophrenia compared to controls. Additionally, the MD thalamus in particular has well-established structural abnormalities in patients with schizophrenia, which have not been observed in the LGN (reviewed in Pergola et al., 2015). And changes in a BOLD fMRI measure of blood flow in the left medial region of the thalamus under high doses of ketamine correlate positively with perceptual distortion symptoms of psychosis (Pollak et al., 2015). Changes in the LGN *have* been observed in schizoaffective and mood disorder patients, so connectivity with this region of thalamus may play a role in negative mood symptoms not usually observed under ketamine (Dorph-Petersen et al., 2008; reviewed in Leivada and Boeckx, 2014). We sought to assess whether NMDA blockade induces connectivity changes in the LGN and MD thalamus in a way that potentially correlates with psychotic symptoms.

2. Materials and methods

2.1. Subjects

Fifty-three subjects (previously reported in Javitt et al., 2018), recruited from three academic research institutions, were medically healthy men and women aged 18 to 55 years old (mean (SD) = 31.1(9.6)) without current or past Axis I or II psychiatric or substance history. Exclusion criteria included: a history of recreational use of ketamine, PCP or other NMDAR modulators; adverse reaction to therapeutic ketamine; first-degree relative with schizophrenia; clinically significant history of violence or suicidality; history of significant medical illness, including high blood pressure (> 140/90); significant neurological illness or head injury; pregnancy; current psychotropic medication use; or color blindness.

2.2. Design

The study was approved by the Local Research Ethics Committees at Yale, Columbia and UC Davis. All subjects gave written informed consent prior to enrollment. Subjects were randomized to ketamine or placebo groups in a 2:1 ratio. More participants were included in the ketamine group in order to increase the range of symptoms for the critical symptom correlation analyses. Subjects participated in two MRI sessions; here we report the results from the resting state fMRI study on infusion day two. Other data for MRS and BOLD task-relevant activation were reported elsewhere (Javitt et al., 2018). The resting scans were acquired 10-min pre and post-ketamine or saline bolus. Clinical assessments were performed following the end of the one-hour infusion. Subjects and clinical researchers were blinded to treatment group. Treatment assignment was randomized and stratified by site so as to minimize site confounds. Demographic information and symptoms induced by ketamine are broken down across site (Table 1).

2.3. Ketamine/placebo infusion

Racemic ketamine hydrochloride (Ketalar; Parke Davis, Morris

Table 1
Demographic data for subjects split into each site where scanning occurred. Symptom Scores and ketamine concentrations also included as mean (standard deviation) values for all subjects receiving ketamine (left) and saline (right) across all three sites. There were significant drug condition by site interaction effects for BPRS-Negative (p = .021), and CADSS-Percept (p = .021) and a main effect of site for CADSS-Percept (0.011). There was also a trending difference across sites for ketamine blood levels (p = .073) but not for nor-ketamine levels (p = .879). Range of possible BPRS scores (20–180), CADSS scores (0–92), POMS (−32−232), BPRS-positive(5–45), BPRS-negative(5–45), and CADSS-perception (0–28).

Site	Yale		CU		UCSD		Overall	
Gender (M/F)	5/4		18/13		8/5		31/22	
Drug condition (K/S)	5/4		20/11		9/4		34/19	
Age, mean (SD), in months	331 (57)		421 (127)		312 (54.8)		379 (114)	
	Ketamine	Saline	Ketamine	Saline	Ketamine	Saline	Ketamine	Saline
Ketamine levels (ng/mL)	139 (63)	N/A	102 (29)	N/A	112 (26)	N/A	111 (31)	N/A
Nor-ketamine levels (ng/mL)	63 (29)	N/A	68 (19)	N/A	68 (15)	N/A	67 (19)	N/A
BPRS	24.0 (10.4)	20.3 (0.5)	23.6 (6.2)	21.3 (1.3)	22.0 (3.0)	20.5 (0.3)	23.2 (5.7)	20.9 (1.2)
CADSS	12.4 (12.7)	2.0 (3.4)	6.2 (7.8)	0.8 (1.8)	6.4 (6.0)	1.5 (1.3)	7.2 (8.2)	1.2 (2.1)
POMS	8.6 (23.8)	−5.8 (9.6)	3.4 (20.6)	−6.9 (13.4)	3.9 (9.6)	3.3 (7.6)	4.3 (18.4)	−4.5 (11.9)
BPRS Negative	7.4 (1.7)	5.0 (0.0)	5.5 (1.2)	5.0 (0.0)	5.6 (0.7)	5.0 (0.0)	5.8 (1.3)	5.0 (0.0)
BPRS Positive	9.6 (3.1)	5.0 (0.0)	6.7 (2.0)	5.0 (0.0)	7.0 (1.7)	5.0 (0.0)	7.2 (2.3)	5.0 (0.0)
CADSS Percept	9.2 (8.8)	0.0 (0.0)	2.8 (3.6)	0.4 (0.9)	3.3 (3.0)	0.0 (0.0)	3.9 (4.9)	0.2 (0.7)

Plains, NJ) was administered [0.23 mg/kg bolus over 1 min followed by 0.58 mg/kg/h over 30 min then 0.29 mg/kg/h over 29 min (D'Souza et al., 2012)] or placebo (saline). This is the highest dose currently in use in psychiatry research with healthy human subjects (D'Souza et al., 2012). Moreover, the paradigm sought to achieve ketamine plasma levels of ~150 ng/mL (Shaffer et al., 2014), associated with moderately high psychotomimetic responses (D'Souza et al., 2012) in the relative absence of sedation, agitation, or other problematic effects. Ketamine and nor-ketamine levels were measured for all subjects given ketamine, except three from Columbia for technical reasons.

2.4. Clinical and safety measures

Subjects were rated with the Brief Psychiatric Rating Scale (BPRS), Profile of Mood States (POMS), and Clinician Administered Dissociative Symptom Scale (CADSS) (Krystal et al., 1994). Sub-scores for positive and negative symptoms were extracted from the BPRS, as well as a "Perception" sub-score from the CADSS (which captures aberrant salience experiences). These were used to analyze the relationship between changes in connectivity and symptoms.

2.5. Scanning parameters

All fMRI scans were conducted on 3 T scanners at Yale University, Columbia University, or University of California at Davis on the following scanners respectively: 3 T Siemens TIM TRIO, 3 T GE MR750, and 3 T Siemens TIM TRIO. All sites used a 32-channel head coil. The same scanning parameters were used across all sites (detailed scanner specifications can be found in Javitt et al., 2018). Briefly, before initial resting state scans, high-resolution T1*weighted anatomical images were acquired for image registration (TR = 1900 ms, TE = 2.98 ms, TI = 1100 ms, matrix = 256 × 256, FOV = 256 mm, voxel size = 1.0 × 1.0 × 1.0mm). Then for both pre-drug baseline and post-drug functional imaging, 32 axial-oblique slices were obtained in an interleaved pattern (TR = 200 ms, TE = 30.0ms, FOV = 220 mm, matrix = 64*64, slice thickness = 4 .0mm, one voxel = 3.4 × 3.4 × 4.0mm).

2.6. Image processing

Images were pre-processed in MNI space and functional connectivity was analyzed in CONN functional connectivity toolbox version 17 (Whitfield-Gabrieli and Nieto-Castanon, 2012; https://www.nitrc.org/projects/conn/), running in Matlab version R2016b (Mathworks, Inc., Natick, MA, USA). The default pre-processing pipeline for volume-based analyses was used with: realignment, slice-timing correction, normalization, ART outlier identification, spatial and temporal filtering, and structural segmentation/normalization to Montreal Neurological Institute (MNI) space. The ART procedure (Whitfield-Gabrieli et al., 2009) was used for artifact detection. Volumes in which the normalized z-scores from global mean signal intensity exceeded 9 or the framewise composite displacement was over 2 mm in x, y or z translations or 0.9 degrees in the pitch, roll or yaw rotations were identified as outliers. These outlier time points, likely caused by head motion, were then regressed out as nuisance covariates and analyses were conducted to determine whether there were differences in various motion parameters across the drug conditions (Table 2). Cerebrospinal fluid (CSF) and white matter (WM) BOLD signal noise were identified via simultaneous normalization/segmentation procedures using posterior probability maps in this normalized space as Gray/White/CSF masks which were thresholded at 0.5 for WM and CSF. Further one-voxel erosion procedures were used to avoid partial volume effects. These masks were then used by the aCompCorr (analytical component-based noise correction; Behzadi et al., 2007) method in this toolbox, to identify and regress out physiological noise in the gray matter regions with the principal component-based noise-correction. This method has been validated as effective in identifying meaningful anti-correlations in resting-state data (Chai et al., 2012). After white matter, CSF, and realignment/motion outlier confounds were removed, BOLD signal despiking was performed using a continuous hyperbolic tangent squashing function in the toolbox to further reduce the influence of outlier scans. Next, images were band-pass filtered using SPM-based Fast Fourier Transformation (FFT) methods (0.0078–0 .1Hz). All EPI-BOLD images were registered to the high-resolution T1*weighted structural images, and then to MNI space. Finally, a 6 mm full-width half-maximum (FWHM) Gaussian kernel was used for smoothing. All correlation coefficients were converted to normally distributed z-scores for first-level analyses to allow for second-level GLM analyses.

Table 2
Means (standard deviations) of the maximum and average framewise displacement due to head motion, as determined by ART procedures, displayed across scanning site and in each drug condition.

	Average subject motion	Maximum subject motion
Site		
Yale	0.03312 (0.0509)	0.309 (0.2437)
Columbia	0.00251 (0.0757)	0.25 (0.2167)
UC-Davis	0.03768 (0.0956)	0.25 (0.1883)
Drug		
Saline	0.0325 (0.0722)	0.313 (0.2586)
Ketamine	0.0187 (0.0884)	0.231 (0.1672)

2.7. Large-scale networks

The large-scale network analyses were conducted between DMN, DAN, FPN and the atlas provided in CONN to parcellate the whole brain into functional sub-regions. The CONN atlas comprises 116 subcortical and cortical regions from the Harvard-Oxford Atlas and 16 cerebellar regions from the AAL atlas.

The ROIs for DMN, FPN DAN and SAL were comprised using 10 mm spheres for the sub-regions of each network (coordinates for each sub-region in Supplemental Table 1; taken from Power et al., 2011, derived from Dosenbach et al., 2007 and Raichle et al., 2001). We combined these sub-regions into a single ROI to establish the respective network masks for DMN, DAN and FPN, with which we explored whole-network dynamics. A false discovery rate (FDR)-correction was applied to all p-values for these four large-scale network analyses separately, and p (FDR) < 0.05 is reported (Benjamini and Hochberg, 1995).

Our follow-up analysis with the salience network also used the combined sub-regions of the network as the seed (coordinates in Supplemental Table 1; taken from White et al., 2010) and included only our DMN, FPN, and DAN ROIs as well as sub-regions of these networks from CONN's default atlas, which were previously determined from an ICA analysis done in CONN using 498 subjects from the Human Connectome Project (https://www.nitrc.org/projects/conn/). The same thresholding procedure was followed.

2.8. DLPFC

The right DLPFC was set as a seed region, and correlations were calculated between this seed and all other voxels in the brain. The coordinates of the 10 mm sphere for this seed are listed in Supplemental Table 1. A voxel-level height threshold of $p < .001$ was applied to these analyses, and then the resulting supra-threshold clusters were reported as significant only with cluster-level false discovery rate (FDR)-corrected p-values $< .05$ (Benjamini and Hochberg, 1995).

2.9. Thalamic nuclei

For the seed-to-voxel analyses of thalamic nuclei, masks were created in SPM Anatomy Toolbox (Eickhoff et al., 2005) using the "visual thalamus" and "MD thalamus" seeds based on functional mapping of the thalamus from Behrens and colleagues (2003). Correlations between these seed regions and all other voxels were calculated. The same thresholding procedure was used for this analysis as the DLPFC.

2.10. Statistical analysis

Two sample *t*-tests were used to assess differences in demographics (sex, race, age) across treatment groups. To ensure our effects were not driven by motion, *t*-test were used to detect differences across drug groups in average and maximum motion realignment parameters (Table 2). Next, one-way ANOVAs were used to assess the difference in clinical measures across site and drug condition (BPRS, CADSS, POMS) using change in score measures (post-infusion minus pre-infusion) with FDR corrections applied.

All connectivity analyses involved *t*-tests on the difference (post-drug minus pre-drug) in z-scored correlations across brain regions between participants given saline versus ketamine. The scanning site was always entered as a covariate in each of these analyses. Effect sizes in the form of standardized beta values are reported, representing the average difference in Fisher-transformed correlation coefficients between drug groups.

2.11. Symptom correlations

All symptom correlations were conducted between symptoms scores of subjects given ketamine and connectivity values across our various regions of interest. Symptom score correlations for the large-scale network analyses were conducted in R Studio (http://www.rstudio.com/). We removed outliers 2 standard deviations from the mean and conducted Spearman rank partial correlations controlling for site with nonparametric permutation tests for significance testing using 10,000 permutations (using the RVAideMemoire package in R; Hervé, 2015). Because of our particular interest in psychotic symptoms, we limited our large-scale network symptom analyses to connectivity between regions previous literature has suggested might be important in positive symptoms of psychosis (Manoliu et al., 2013; Pollak et al., 2015; Raji et al., 2015). This included connectivity of the DMN with DAN and FPN, as well as our large-scale network connectivity with the putamen and thalamus, which also seem to have important functional connections for regulating DMN and task-positive network dynamics (Di and Biswal, 2014). Then FDR-correction was applied to p-values, and only p (FDR) < 0.05 was reported.

For the DLPFC and thalamic-seed symptom correlation analyses, we did partial correlations in subjects given ketamine, controlling for site with nonparametric, permutation tests with 1000 iterations. A voxel-level height threshold of $p < .001$ was applied to the whole brain and then results of cluster-level p(FDR) < 0.05 were reported.

3. Results

3.1. Sample

Subjects showed no group differences for average age (p (FDR) = 0.70) or gender distribution (p(FDR) = 0.18) based on drug assignment (34 ketamine/19 placebo). No serious or unexpected adverse events were reported in the study. Ketamine levels were on average 110 ng/mL, which was significantly lower than the target 150 ng/mL blood concentration (p(FDR) < 0.001; blood levels reported across sites in Table 1).

3.2. Clinical ratings

CADSS, BPRS and POMS scores were greater under ketamine compared to saline (main effect of drug condition: p(FDR) = 0.006, 0.03 and 0.019). The BPRS positive (p(FDR) = 0.0001), BPRS-negative (p (FDR) = 0.010 and CADSS-perceptual (p(FDR) = 0.0002) subscales also showed significant changes across ketamine and saline participants.

3.3. Covariates

There were no differences in average (p(FDR) = 0.564) nor maximum (p(FDR) = 0.33) head motion between the drug conditions. There also were no significant gender differences for any connectivity measure of interest in our analyses (p(FDR) > 0.33). Our analyses for differences in connectivity across the three sites revealed no effect of site for DLPFC, LGN, or any of the large-scale networks. However, the connectivity between MD thalamus and a cluster of voxels in superior temporal cortex did show a significant effect of site (coordinates: 52, −46, 14; 115 voxels; p(FDR) = 0.0281). This region overlapped with a region that showed significant differences across saline and ketamine (see below) however the effect of ketamine survived when controlling for site in these analyses. There were differences in symptoms evinced by the ketamine treatment across sites (see Table 1), which could possibly be related to a trending difference in ketamine concentrations (p = .073) (but not nor-ketamine concentration (p = .88)) across site. This is why site was included as a covariate in our imaging as well as symptom correlation analyses.

3.4. Large-scale network connectivity

In our DMN/DAN/FPN large-scale network analyses, we did not

Table 3
Statistics including Fisher-transformed connectivity mean (standard deviation) values, *t*-value, standardized Beta, and FDR-corrected p-value in each cluster identified by seed-to-voxel and large-scale network analyses comparing saline and ketamine. All *t*-values and p(FDR)-corrected values for symptom correlations not reported in text. Beta values are standardized. Coordinates (MNI) and size of cluster also given for seed-to voxel analyses.

Analysis/Region	Size	X	Y	Z	Mean (SD)	Statistics (if not reported in text)
Large-scale networks						
DMN-ACC	–	–	–	–	K: 0.168 (0.247) S: 0.103 (0.167)	$t_{(49)}$ = 4.97, Beta = 0.580, p(FDR) = 0.0012
DMN-PCC	–	–	–	–	K: 0.644 (0.260) S: 0.596 (0.236)	$t_{(49)}$ = 3.66, Beta = 0.463, p(FDR) = 0.0228
DMN-L Nuc Accumbens	–	–	–	–	K: −0.146 (0.370) S: 0.070 (0.129)	$t_{(49)}$ = 3.20, Beta = 0.416, p(FDR) = 0.0486;
DMN-L Insula	–	–	–	–	K: −0.043 (0.188) S: −0.127 (0.185)	$t_{(49)}$ = 4.34, Beta = 0.527, p(FDR) = 0.0051
DMN-R Insula	–	–	–	–	K: −0.070 (0.177) S: −0.125 (0.176)	$t_{(49)}$ = 3.65, Beta = 0.462, p(FDR) = 0.0228
DMN-R Paracing Gyrus	–	–	–	–	K: 0.498 (0.252) S: 0.427 (0.211)	$t_{(49)}$ = 3.21, Beta = 0.417, p(FDR) = 0.0486
DMN-R Frontal Pole	–	–	–	–	K: 0.489 (0.225) S: 0.496 (0.206)	$t_{(49)}$ = 3.29, Beta = 0.425, p(FDR) = 0.0486
SAL-DMN	–	–	–	–	K: 0.260 (0.195) S: −0.074 (0.236)	$T_{(49)}$ = 5.59, Beta = 0.624, p(FDR) = 0.000045
SAL-L PFC (FPN)	–	–	–	–	K: 0.133 (0.212) S: −0.110 (0.223)	$T_{(49)}$ = 3.73, Beta = 0.470, p(FDR) = 0.0038
SAL-R Lateral Parietal (DMN)	–	–	–	–	K: 0.154 (0.185) S: −0.065 (0.238)	$T_{(49)}$ = 3.51, Beta = 0.448, p(FDR) = 0.0049
SAL-R Posterior Parietal Cortex (FPN)	–	–	–	–	K: 0.142 (0.207) S: −0.025 (0.222)	$T_{(49)}$ = 2.80, Beta = 0.371, p(FDR) = 0.0274
DLPFC						
R Post-central gyrus	127	32	−42	64	K: 0.115 (0.166) S: −0.083 (0.162)	$t_{(51)}$ = 4.44, Beta = 0.528, p(FDR) = 0.043
Pons	127	4	−18	−46	K: −0.064 (0.097) S: 0.128 (0.127)	$t_{(51)}$ = −5.96, Beta = −0.641, p(FDR) = 0.043
MD Thalamus						
R Superior temporal gyrus	251	42	−40	10	K: 0.197 (0.124) S: 0.004 (0.147)	$t_{(51)}$ = 5.69, Beta = 0.623, p(FDR) < 0.001
R Parahippocampal gyrus	124	18	−10	−28	K: 0.157 (0.105) S: −0.052 (0.158)	$t_{(51)}$ = 5.82, Beta = 0.632, p(FDR) = 0.025
Symptom correlations						
DLPFC-POMS						
L Frontal Orbital Cortex	217	−26	24	−8		$t_{(51)}$ = 5.77, Beta = 0.640, p(FDR) = 0.038
ACC	197	4	38	20		$t_{(51)}$ = 5.27, Beta = 0.605, p(FDR) = 0.038

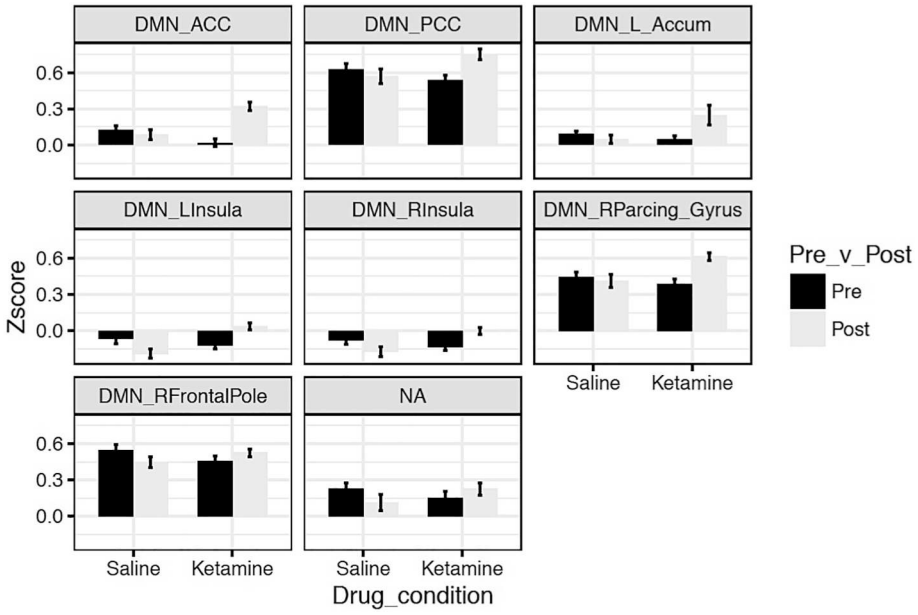

Fig. 1. Altered connectivity between DMN and various regions of interest in participants given ketamine versus saline. Bars represent average *Z*-score of correlation, error bars are standard error. All post-pre difference scores are significantly different across drug condition, p(FDR) < 0.05.

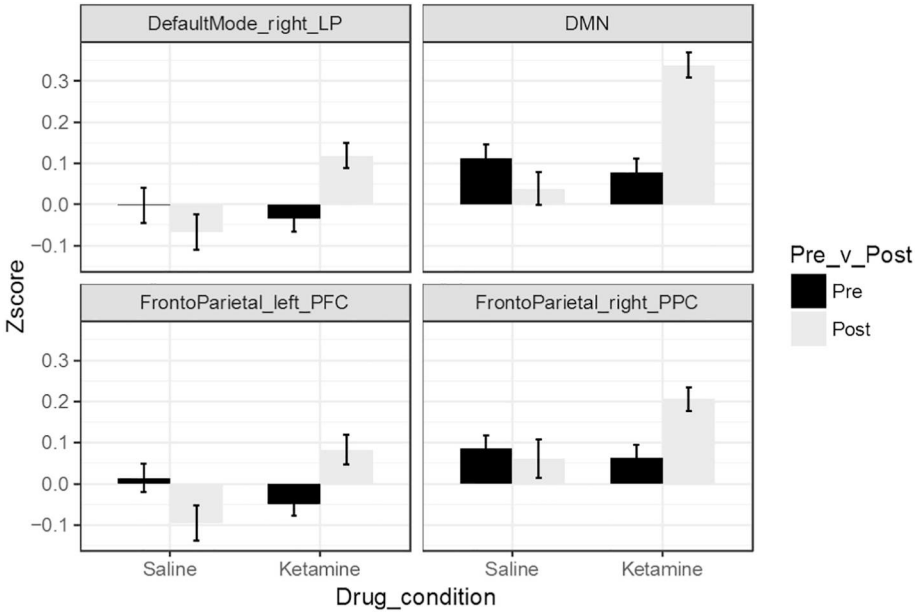

Fig. 2. Altered connectivity between SAL and subregions of the FPN and DMN in participants given ketamine versus saline. Bars represent average Z-score of correlation, error bars are standard error. All difference scores are significantly different across drug condition, p(FDR) < 0.05.

find any effect of ketamine compared to saline on DMN-DAN connectivity (p(FDR) = 0.980) or DMN-FPN connectivity (p(FDR) = 0.0742). However, ketamine increased the correlation between the DMN and a range of regions across the cortex and striatum compared to saline (Table 3) including the anterior cingulate cortex (ACC) (Fig. 1a), posterior cingulate cortex (PCC) (Fig. 1b), left nucleus accumbens (Fig. 1c), bilateral insula (Fig. 1d and e), right paracingulate gyrus (Fig. 1f) and right frontal pole (Fig. 1g).

Our results showed changes between the large-scale networks and regions of the salience network, which has previously been implicated as important for modulating the relationship between task positive and default mode networks (Chen et al., 2013; Zhou et al., 2018) and dysfunction in this relationship has been implicated in schizophrenia (Manoliu et al., 2013; Wotruba et al., 2014). Therefore, we followed up with a direct analysis of the differences in connectivity between the salience network and our default mode and task positive networks. Our findings showed that connectivity between the salience network and whole DMN seed was increased under ketamine, at least in part driven by significant differences in the right lateral parietal seed in the DMN (Table 3; Fig. 2). There were also increases in salience network connectivity with regions of the FPN, including right posterior parietal cortex and left prefrontal cortex under ketamine (Table 3; Fig. 2).

3.5. DLPFC connectivity

When looking more closely at the dorsolateral PFC within the FPN, we found that connectivity with the DLPFC was disrupted by ketamine in a cluster of voxels in the right post-central gyrus and in the pons (Fig. 3; Table 3). None of the regions differentially connected with DLPFC under ketamine were part of the DMN or DAN.

3.6. Thalamic nuclei connectivity

Our analyses with the two sub-nuclei of the thalamus (LGN and MD, which exhibit aberrant connectivity in schizophrenia (Anticevic et al., 2014a)), revealed that the MD thalamus evinced increased connectivity with the right superior temporal gyrus in participants given ketamine versus saline (Table 3; Fig. 4). Part of the right parahippocampal gyrus also showed increased connectivity with the MD nucleus under ketamine. But no differences were found between the saline and ketamine groups for the connectivity between the LGN seed and any other voxels in the brain.

3.7. Symptom correlations

3.7.1. Large-scale networks

Given our interest in ketamine's use as a tool to elicit symptoms of psychosis, we investigated how functional connectivity between our network ROIs and regions of thalamus and striatum under ketamine correlated with positive symptom ratings. None of the regions of interest we selected showed a significant relationship with positive symptoms induced under ketamine (p(FDR) > 0.35).

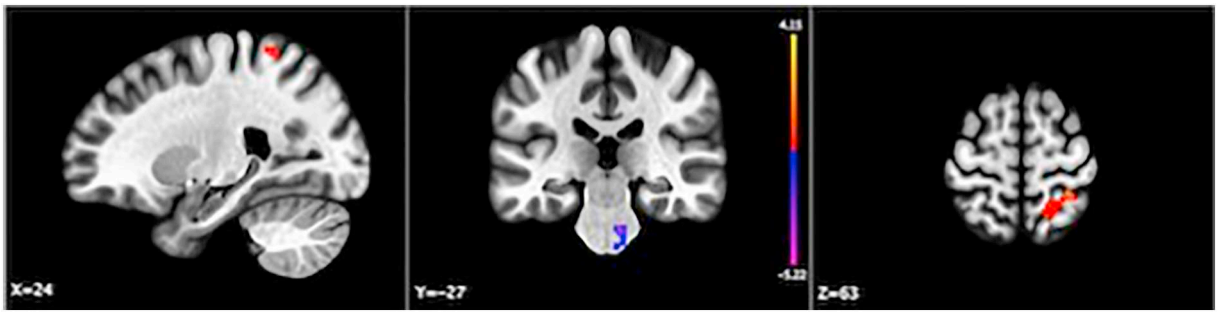

Fig. 3. Clusters with significantly different connectivity with the DLPFC in participants given ketamine versus saline. Color bar indicates *t*-value; p(FDR) < 0.05.

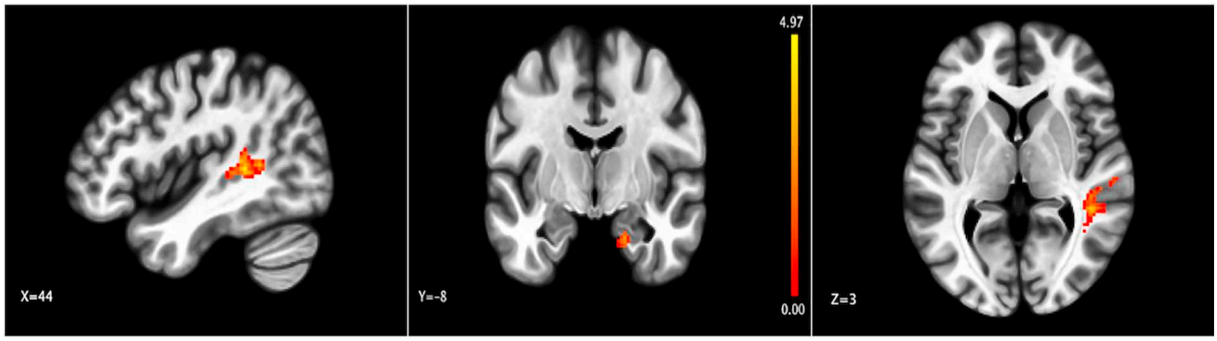

Fig. 4. Changes in connectivity with the MD thalamus. Representation of areas where connectivity with MD thalamus was altered in participants given ketamine compared to control. Color bar represents *t*-value; p(FDR) < 0.05.

3.7.2. DLPFC-seed

POMS mood scores correlated with DLPFC connectivity with ACC as well as a region of left frontal orbital cortex connectivity (Table 3).

3.7.3. Thalamic seeds

Functional connectivity with the MD nucleus of the thalamus did not correlate with any symptom scores in participants given ketamine.

4. Discussion

Our results did not reveal an effect of ketamine compared to saline on DMN-FPN or DMN-DAN connectivity during rest, an effect previously shown in patients with schizophrenia (Whitfield-Gabrieli et al., 2009; Gerretsen et al., 2014) and in participants given ketamine during a WM task (Anticevic et al., 2012). Mueller et al. (2018) similarly found no change in DLPFC connectivity with regions of DMN with a lower dose of ketamine at rest. Although, a dose of ketamine that achieved blood levels over six times those observed in this study did find altered DMN-TPN connectivity (Bonhomme et al., 2016), so it is possible these large-scale network effects are dose-dependent.

In our study, connectivity between the DMN and ACC, insula, PCC, nucleus accumbens, paracingulate cortex and frontal pole all increased under ketamine compared to saline. The insula is well-placed to influence the balance between bottom-up and top-down processing in predictive coding schemes (Chanes and Barrett, 2016), which has been linked to perceptual distortions in schizophrenia (Powers III et al., 2016).

Notably, the insula and ACC make up the salience network (SAL), a cluster of regions whose connectivity has been shown through effective connectivity analyses to dampen DMN activity and modulate the connectivity between DMN and DAN/FPN in healthy participants (Chen et al., 2013; Zhou et al., 2018), which have both been shown previously to be disrupted under ketamine during similar WM tasks (Anticevic et al., 2012). This motivated us to follow-up with explicit tests of the relationship between the salience network and DMN, DAN and FPN, which revealed an effect of ketamine on connectivity between salience network and regions of both the DMN and FPN. Interestingly, hypo-connectivity between the DMN and SAL has been consistently shown in patients with schizophrenia compared to controls (Manoliu et al., 2013; reviewed in Nekovarova et al., 2014), while our analyses revealed hyper-connectivity amongst these regions. This difference from the effects we found under ketamine could be related to illness course. Previous research has shown ketamine models functional connectivity in first-episode participants better than in chronic patients, and these two patient groups can show opposite patterns of connectivity within the same region (Anticevic et al., 2015a). Youth at risk of psychosis do show decreased anti-correlation between DMN and SAL, which is consistent with our current results under ketamine (Wotruba et al., 2014; see Table 4 for a summary of these results across disease progression in relation to our results).

Additionally, the PCC and frontal pole are both regions within the DMN, so their altered correlation with our whole DMN seed represents disruptions in intrinsic connectivity within this network at rest under ketamine versus saline. This coincides with previous research demonstrating that patients with schizophrenia have internal hyper-connectivity within DMN nodes, which correlated with positive symptoms (Whitfield-Gabrieli et al., 2009).

Although our dose of ketamine during rest did not induce significant changes in the DMN-DAN/FPN connectivity, we do see changes in connectivity between these large-scale networks and many regions believed to control the anti-correlation between them (insula, ACC) (Di and Biswal, 2014; Chen et al., 2013; Zhou et al., 2018); a task condition (Anticevic et al., 2012) or higher dose of ketamine (Bonhomme et al., 2016) may be necessary to elicit disrupted anti-correlations between these networks.

Mueller et al. (2018) previously found altered connectivity within-subjects under ketamine versus saline between the DLPFC and ACC, superior frontal gyrus and calcarine fissure, which we did not observe with our higher ketamine dose. We did find a relationship between DLPFC-ACC connectivity and mood symptoms so this may be relevant to this change observed by Mueller and colleagues under ketamine versus saline. Additionally, in line with our large-scale network results and Mueller and colleagues' findings (2018), the right DLPFC within the FPN did not show altered connectivity with any regions within the DMN under ketamine versus saline. This specific region within the FPN usually evinces the greatest alterations in connectivity with DMN seeds in patients (Whitfield-Gabrieli et al., 2009); these results together support our conclusion that unlike in schizophrenia, during resting state conditions the alterations in DMN-FPN connectivity are not present or are too weak to reach statistical significance under various sub-anesthetic doses of ketamine. The DLPFC time series showed altered coupled with the ACC in a way that positively correlated with changes in subjects' mood reports as measured by POMS. While the POMS is a crude measure of mood, these relationships could be relevant to the psychotomimetic and potential antidepressant effects of ketamine. This fits well with previous ideas about the role of the prefrontal cortex connectivity in mood disorders and in ketamine's ability to alleviate these symptoms (Abdallah et al., 2014). The ACC has also been strongly implicated in mood disorders previously (reviewed in Drevets et al., 2008) and in ketamine's (and other NMDA antagonists that do not induce psychotic symptoms) early sites of action for its antidepressant effects (Downey et al., 2016). Further work is needed to explicitly explore these diverging pathways that may be involved in ketamine's effect on mood versus psychosis.

Ketamine has been shown to alter blood flow to the thalamus in a way that correlates with perceptual alterations induced by this drug (Pollak et al., 2015), but to our knowledge nobody has ever looked at specific patterns of thalamic nuclei connectivity in relation to these symptoms. Our results showed various changes in connectivity with MD thalamus. Changes in several structural and synaptic measures have

Table 4
Findings from previous studies of participants with schizophrenia in at-risk, first episode or chronic phases in relation to our results with participants given ketamine.

Study	Patient group (Chronic, first-episode or at-risk schizophrenia)	Schizophrenia findings	Our findings with ketamine
Thalamus			
Anticevic et al., 2014a	Chronic	Increased connectivity with sensory cortices; decreased connectivity with PFC, striatum and cerebellum	- Increased connectivity with primary sensory cortex (auditory);
Anticevic et al., 2014b	Chronic	Over-connectivity with sensory-motor regions; decreased connectivity with striatum, prefrontal and cerebellar regions	- Increased connectivity with parahippocampal gyrus;
Ferri et al., 2018	Chronic	Decreased connectivity with cerebellum and ACC; Increased connectivity with regions of visual and auditory cortex, precentral gyrus and lingual gyrus	- No regions of decreased connectivity found
Anticevic et al., 2015b	At-risk	Increased connectivity with sensory cortices; decreased connectivity with PFC, striatum, and cerebellum (especially in future converters)	
PFC			
Anticevic et al., 2015a	First-episode	Increased medial PFC global connectivity	- Increased dorsolateral connectivity with post-central gyrus;
Anticevic et al., 2015a	Chronic	Reduced lateral PFC global connectivity	- Decreased DLPFC connectivity with pons.
Large-scale networks			
Whitfield-Gabrieli et al., 2009	Chronic	Increased within-DMN connectivity; Decreased anticorrelation between DMN and right DLPFC	- Increased connectivity between DMN and Salience network, as well as regions of FPN and
Manoliu et al., 2013	Chronic	Decreased SAL-DMN/CEN connectivity (esp dorsal CEN and superior-posterior DMN)	Salience network; - Increased within-DMN connectivity;
Wotruba et al., 2014	At-risk	Increased connectivity (decreased anticorrelation) between regions of DMN and task positive network; Increased connectivity (decreased anticorrelation) between DMN and SAL regions	- DMN connectivity also increase with other regions of striatum, and paracingulate gyrus; - No specific changes in right DLPFC or DAN/FPN
Du et al., 2018	At-risk and first-episode	Regionally specific hypo- and hyper-connectivity in large-scale networks were similar but fewer/smaller regions in at-risk compared to chronic patients.	connectivity with DMN
Whole brain			
Li et al., 2017	Chronic	Alterations in frontal cortex connectivity (mostly increased); changes in thalamic connectivity and other subcortical and limbic patterns of connectivity	- No explicit whole brain analyses for frontal cortex analyses. - Some thalamic changes replicated with sensory
Li et al., 2017	First-episode	Alterations in frontal cortex connectivity (mostly increased)	cortices; - Frontal lobe connectivity increased with DMN

been discovered specifically in the MD nucleus of the thalamus in schizophrenia (reviewed in Pergola et al, 2015), while the LGN may be more involved in negative mood symptoms (Dorph-Petersen et al., 2008; reviewed in Leivada and Boeckx, 2014), so it is not surprising that ketamine elicited altered functional dynamics in the MD thalamus as opposed to LGN. And this demonstrates that the functional effects of ketamine are specific to certain sub-regions of the thalamus as opposed to the entire structure. Prior studies demonstrate that patients with schizophrenia have deficits in thalamic connectivity with association cortices, and hyper-connectivity with sensorimotor and sensory cortices (Anticevic et al., 2014a; Anticevic et al., 2014b; Anticevic et al., 2015b). Our data indicates somewhat different but overlapping patterns of altered thalamic connectivity with ketamine. We found increased mediodorsal thalamic functional connectivity with areas involved in auditory processing in the superior temporal gyrus (in line with previous work), and with parahippocampal gyrus, but no altered connectivity between the LGN and sensorimotor cortices. We also did not find MD thalamus to PFC changes as seen in patients with schizophrenia (Anticevic et al., 2014a; Anticevic et al., 2014b; Anticevic et al., 2015b; see Table 4 see Table 4 for a summary of these results across disease progression in relation to our results).

Finally, we tested for symptom correlations with positive symptom and mood scales, and did not find any significant relationships between our measures of connectivity in the a priori ROIs and positive symptoms of schizophrenia. This is in line with previous research (Mueller et al., 2018) showing ketamine changes relevant to large-scale task positive and default mode network dynamics do not correlate with positive symptoms. It is possible the changes across drug conditions we observed are more relevant to cognitive and working memory deficits, which were not tested in the present study.

4.1. Limitations

There are a few limitations that should be noted when interpreting the results of this study. First, the design was a between-subjects design with a baseline scan, which may be less powerful than a within-subjects design with a placebo and ketamine scan. This could have driven some of the differences between the present results and previous studies (Mueller et al., 2018). Second, although the multi-site nature of the study is useful for showing effects of ketamine that are reliable across scanning location, we did see some differences across sites especially related to symptom scores and ketamine blood levels. We controlled for site in all of our analyses to try to account for these differences.

Next, there has been little evidence for the stability of reported CADSS, POMS and BPRS scores following ketamine administration. One study does suggest the CADSS scale has high sensitivity for ketamine's effects but low Interclass Correlations across infusions within-subject (De Simoni et al., 2013). CADSS scores may not be stable with ketamine infusion, however most of our symptom correlations occur with both BPRS and CADSS subscales with overlapping symptoms measured, suggesting the scales are producing a consistent measure of the participant's experience in our study.

4.2. Conclusions

We sought to investigate the effects of ketamine on functional connectivity using seeds of interest previously identified in patients with schizophrenia. We did find alterations consistent with those observed in patients with schizophrenia, including hyper-connectivity between MD thalamus and sensory cortical regions, as well as increased intra-network connectivity within the DMN. We also provide further support that ketamine may model some fc patterns of early or at-risk

patients with psychotic illnesses better than chronic schizophrenia patients (Anticevic et al., 2015a). We provide a table comparing the results we saw under ketamine with previous results reported in patients with schizophrenia across different stages of illness progression (Table 4). Unsurprisingly, ketamine does not replicate all of the findings from patients with schizophrenia, including altered large-scale network dynamics at rest and thalamic-PFC connectivity. Importantly our results identify possible causal relationships between NMDA signaling disruptions and various alterations in patterns of DMN, thalamic, superior temporal cortical and insular connectivity, which have also been observed in patients with schizophrenia. These signatures may serve as important biomarkers for future work with the use of ketamine as a model of these symptoms, and in understanding ketamine-induced psychosis and psychotic illnesses more generally.

Declarations of interest

Dr. Javitt has received consulting payments or honoraria from Forum, Takeda, Pfizer, Autifony, Glytech, and Lundbeck; has served on the scientific advisory board for Promentis and Phytonics; holds equity in Glytech, AASI, and NeuroRx; and holds intellectual property for use of by *N*-methyl-D-aspartate receptor agonists in schizophrenia and movement disorders as well as by *N*-methyl-D-aspartate receptor antagonists in depression, obsessive-compulsive disorder, and posttraumatic stress disorder. Dr. Krystal has served as a consultant for AstraZeneca, Biogen, Biomedisyn, Janssen, LEK Otsuka, Pragma Therapeutics, SK Life Science, Spring Care, Sunovion, Takeda, Taisho, and Teva; has received research support from AstraZeneca and Pfizer; has served on scientific advisory boards for biOasis Technologies, Biohaven Pharmaceuticals, Blackthorn Therapeutics, Broad Institute, Lohocla Research Corporation, Luc Therapeutics, Pfizer, and TRImaran Pharma; holds equity in Biohaven Pharmaceuticals, Blackthorn Therapeutics, Luc Therapeutics, and Spring Care; and holds intellectual property for glutamate modulating agents in treatment of mental disorders and intranasal ketamine for treatment of depression. No other disclosures were reported by any other authors.

Acknowledgements

This study was supported by government contract HHSN271201200007I to the New York State Psychiatric Institute and the Research Foundation for Mental Hygiene from the National Institute of Mental Health. This work was also supported by NIH Training Grant T32 NS41228 funded by the Jointly Sponsored NIH Predoctoral Training Program in the Neurosciences.

Appendix A. Supplementary data

Supplementary data to this article can be found online at https://doi.org/10.1016/j.nicl.2019.101739.

References

Abdallah, C.G., Sanacora, G., Duman, R.S., Krystal, J.H., 2014. Ketamine and rapid-acting antidepressants: a window into a new neurobiology for mood disorder therapeutics. Annu. Rev. Med. 66, 509–523.

Anticevic, A., Corlett, P.R., 2012. Cognition-emotion dysinteraction in schizophrenia. Front. Psychol. 3, 392. https://doi.org/10.3389/fpsyg.2012.00392.

Anticevic, A., Gancsos, M., Murray, J.D., Repovs, G., Driesen, N.R., Ennis, D.J., ... Corlett, P.R., 2012. NMDA receptor function in large-scale anticorrelated neural systems with implications for cognition and schizophrenia. Proc. Natl. Acad. Sci. U. S. A. 109 (41), 16720–16725. https://doi.org/10.1073/pnas.1208494109.

Anticevic, A., Cole, M.W., Repovs, G., Murray, J.D., Brumbaugh, M.S., Winkler, A.M., ... Glahn, D.C., 2014a. Characterizing thalamo-cortical disturbances in schizophrenia and bipolar illness. Cereb. Cortex 24 (12), 3116–3130. https://doi.org/10.1093/cercor/bht165.

Anticevic, A., Yang, G., Savic, A., Murray, J.D., Cole, M.W., Repovs, G., ... Glahn, D.C., 2014b. Mediodorsal and visual thalamic connectivity differ in schizophrenia and bipolar disorder with and without psychosis history. Schizophr. Bull. 40 (6), 1227–1243. https://doi.org/10.1093/schbul/sbu100.

Anticevic, A., Corlett, P.R., Cole, M.W., Savic, A., Gancsos, M., Tang, Y., ... Krystal, J.H., 2015a. N-methyl-D-aspartate receptor antagonist effects on prefrontal cortical connectivity better model early than chronic schizophrenia. Biol. Psychiatry 77 (6), 569–580. https://doi.org/10.1016/j.biopsych.2014.07.022.

Anticevic, A., Haut, K., Murray, J.D., Repovs, G., Yang, G.J., Diehl, C., ... Cannon, T.D., 2015b. Association of thalamic dysconnectivity and conversion to psychosis in youth and young adults at elevated clinical risk. JAMA Psychiatry 72 (9), 882–891. https://doi.org/10.1001/jamapsychiatry.2015.0566.

Balu, D.T., 2016. The NMDA receptor and schizophrenia: from pathophysiology to treatment. Adv. Pharmacol. 76, 351–382. https://doi.org/10.1016/bs.apha.2016.01.006.

Behrens, T.E., Johansen-Berg, H., Woolrich, M.W., Smith, S.M., Wheeler-Kingshott, C.A.M., Boulby, P.A., ... Thompson, A.J., 2003. Non-invasive mapping of connections between human thalamus and cortex using diffusion imaging. Nat. Neurosci. 6 (7), 750.

Behzadi, Y., Restom, K., Liau, J., Liu, T.T., 2007. A component based noise correction method (CompCor) for BOLD and perfusion based fMRI. Neuroimage 37 (1), 90–101. https://doi.org/10.1016/j.neuroimage.2007.04.042.

Benjamini, Y., Hochberg, Y., 1995. Controlling the false discovery rate: a practical and powerful approach to multiple testing. J. R. Stat. Soc. Ser. B Methodol. 57 (1), 289–300.

Bonhomme, V., Vanhaudenhuyse, A., Demertzi, A., Bruno, M., Jaquet, O., Bahri, M.A., Plenevaux, A., Boly, M., Boveroux, P., Soddu, A., Brichant, J.F., Maquet, P., Laureys, S., 2016. Resting-state network-specific breakdown of functional connectivity during ketamine alteration of consciousness in volunteers. Anesthesiology 125 (5), 873–888. https://doi.org/10.1097/ALN.0000000000001275.

Chai, X.J., Castañón, A.N., Öngür, D., Whitfield-Gabrieli, S., 2012. Anticorrelations in resting state networks without global signal regression. NeuroImage 59 (2), 1420–1428. https://doi.org/10.1016/j.neuroimage.2011.08.048.

Chanes, L., Barrett, L.F., 2016. Redefining the role of limbic areas in cortical processing. Trends Cogn. Sci. 20 (2), 96–106. https://doi.org/10.1016/j.tics.2015.11.005.

Chen, A.C., Oathes, D.J., Chang, C., Bradley, T., Zhou, Z.W., Williams, L.M., ... Etkin, A., 2013. Causal interactions between fronto-parietal central executive and default-mode networks in humans. Proc. Natl. Acad. Sci. U. S. A. 110 (49), 19944–19949. https://doi.org/10.1073/pnas.1311772110.

Corlett, P.R., Honey, G.D., Aitken, M.R., Dickinson, A., Shanks, D.R., Absalom, A.R., ... Fletcher, P.C., 2006. Frontal responses during learning predict vulnerability to the psychotogenic effects of ketamine: linking cognition, brain activity, and psychosis. Arch. Gen. Psychiatry 63 (6), 611–621. https://doi.org/10.1001/archpsyc.63.6.611.

Corlett, P.R., Honey, G.D., Fletcher, P.C., 2007a. From prediction error to psychosis: ketamine as a pharmacological model of delusions. J. Psychopharmacol. 21 (3), 238–252. https://doi.org/10.1177/0269881107077716.

Corlett, P.R., Murray, G.K., Honey, G.D., Aitken, M.R., Shanks, D.R., Robbins, T.W., Bullmore, E.T., Dickinson, A., ... Fletcher, P.C., 2007b. Disrupted prediction-error signal in psychosis: evidence for an associative account of delusions. Brain 130 (Pt 9), 2387–2400.

De Simoni, S., Schwarz, A.J., O'Daly, O.G., Marquand, A.F., Brittain, C., Gonzales, C., ... Mehta, M.A., 2013. Test–retest reliability of the BOLD pharmacological MRI response to ketamine in healthy volunteers. Neuroimage 64, 75–90.

Di, X., Biswal, B.B., 2014. Modulatory interactions between the default mode network and task positive networks in resting-state. PeerJ 2, e367.

Dorph-Petersen, K.A., Caric, D., Saghafi, R., Zhang, W., Sampson, A.R., Lewis, D.A., 2008. Volume and neuron number of the lateral geniculate nucleus in schizophrenia and mood disorders. Acta Neuropathol. 117 (4), 369–384.

Dosenbach, N.U., Fair, D.A., Miezin, F.M., Cohen, A.L., Wenger, K.K., Dosenbach, R.A., ... Petersen, S.E., 2007. Distinct brain networks for adaptive and stable task control in humans. Proc. Natl. Acad. Sci. U. S. A. 104 (26), 11073–11078. https://doi.org/10.1073/pnas.0704320104.

Downey, D., Dutta, A., McKie, S., Dawson, G.R., Dourish, C.T., Craig, K., ... Williams, S., 2016. Comparing the actions of lanicemine and ketamine in depression: key role of the anterior cingulate. Eur. Neuropsychopharmacol. 26 (6), 994–1003.

Drevets, W.C., Savitz, J., Trimble, M., 2008. The subgenual anterior cingulate cortex in mood disorders. CNS Spectrums 13 (8), 663.

Driesen, N.R., McCarthy, G., Bhagwagar, Z., Bloch, M., Calhoun, V., D'Souza, D.C., ... Krystal, J.H., 2013a. Relationship of resting brain hyperconnectivity and schizophrenia-like symptoms produced by the NMDA receptor antagonist ketamine in humans. Mol. Psychiatry 18 (11), 1199–1204. https://doi.org/10.1038/mp.2012.194.

Driesen, N.R., McCarthy, G., Bhagwagar, Z., Bloch, M.H., Calhoun, V.D., D'Souza, D.C., ... Krystal, J.H., 2013b. The impact of NMDA receptor blockade on human working memory-related prefrontal function and connectivity. Neuropsychopharmacology 38 (13), 2613–2622. https://doi.org/10.1038/npp.2013.170.

D'Souza, D.C., Ahn, K., Bhakta, S., Elander, J., Singh, N., Nadim, H., ... Ranganathan, M., 2012. Nicotine fails to attenuate ketamine-induced cognitive deficits and negative and positive symptoms in humans: implications for schizophrenia. Biol. Psychiatry 72 (9), 785–794. https://doi.org/10.1016/j.biopsych.2012.05.009.

Du, Y., Fryer, S.L., Lin, D., Sui, J., Yu, Q., Chen, J., ... Mathalon, D.H., 2018. Identifying functional network changing patterns in individuals at clinical high-risk for psychosis and patients with early illness schizophrenia: a group ICA study. NeuroImage 17, 335–346. https://doi.org/10.1016/j.nicl.2017.10.018.

Eickhoff, S.B., Stephan, K.E., Mohlberg, H., Grefkes, C., Fink, G.R., Amunts, K., Zilles, K., 2005. A new SPM toolbox for combining probabilistic cytoarchitectonic maps and functional imaging data. Neuroimage 25 (4), 1325–1335.

Ferri, J., Ford, J.M., Roach, B.J., Turner, J.A., van Erp, T.G., Voyvodic, J., ... Mathalon, D.H., 2018. Resting-state thalamic dysconnectivity in schizophrenia and relationships with symptoms. Psychol. Med. 1–8. https://doi.org/10.1017/S003329171800003X.

Frohlich, J., Van Horn, J.D., 2013. Reviewing the ketamine model for schizophrenia. J. Psychopharmacol. (Oxford, Engl.) 28 (4), 287–302.
Gerretsen, P., Menon, M., Mamo, D.C., Fervaha, G., Remington, G., Pollock, B.G., Graff-Guerrero, A., 2014. Impaired insight into illness and cognitive insight in schizophrenia spectrum disorders: resting state functional connectivity. Schizophr. Res. 160 (1–3), 43–50. https://doi.org/10.1016/j.schres.2014.10.015.
Haaf, M., Leicht, G., Curic, S., Mulert, C., 2018. Glutamatergic deficits in schizophrenia - biomarkers and pharmacological interventions within the ketamine model. Curr. Pharm. Biotechnol. 19 (4), 293–307.
Hervé, M., 2015. RVAideMemoire: Diverse Basic Statistical and Graphical Functions. R package version 0.9-45-2. Available at. http://CRAN.R-project.org/package=RVAideMemoire.
Javitt, D.C., Carter, C.S., Krystal, J.H., Kantrowitz, J.T., Girgis, R.R., Kegeles, L.S., ... Lieberman, J.A., 2018. Utility of imaging-based biomarkers for glutamate-targeted drug development in psychotic disorders: a randomized clinical trial. JAMA Psychiatry 75 (1), 11–19. https://doi.org/10.1001/jamapsychiatry.2017.3572.
Krystal, J.H., Karper, L.P., Seibyl, J.P., Freeman, G.K., Delaney, R., Bremner, J.D., ... Charney, D.S., 1994. Subanesthetic effects of the noncompetitive NMDA antagonist, ketamine, in humans. Psychotomimetic, perceptual, cognitive, and neuroendocrine responses. Arch. Gen. Psychiatry 51 (3), 199–214.
Krystal, J.H., D'Souza, D.C., Mathalon, D., Perry, E., Belger, A., Hoffman, R., 2003. NMDA receptor antagonist effects, cortical glutamatergic function, and schizophrenia: toward a paradigm shift in medication development. Psychopharmacology 169 (3), 215–233. https://doi.org/10.1007/s00213-003-1582-z.
Krystal, J.H., Anticevic, A., Yang, G.J., Dragoi, G., Driesen, N.R., Wang, X.J., Murray, J.D., 2017. Impaired tuning of neural ensembles and the pathophysiology of schizophrenia: a translational and computational neuroscience perspective. Biol. Psychiatry 81 (10), 874–885. https://doi.org/10.1016/j.biopsych.2017.01.004.
Lefort-Besnard, J., Bassett, D.S., Smallwood, J., Margulies, D.S., Derntl, B., Gruber, O., ... Bzdok, D., 2018. Different shades of default mode disturbance in schizophrenia: subnodal covariance estimation in structure and function. Hum. Brain Mapp. 39 (2), 644–661. https://doi.org/10.1002/hbm.23870.
Leivada, E., Boeckx, C., 2014. Schizophrenia and cortical blindness: protective effects and implications for language. Front. Hum. Neurosci. 8, 940. https://doi.org/10.3389/fnhum.2014.00940.
Li, T., Wang, Q., Zhang, J., Rolls, E.T., Yang, W., Palaniyappan, L., ... Feng, J., 2017. Brain-wide analysis of functional connectivity in first-episode and chronic stages of schizophrenia. Schizophr. Bull. 43 (2), 436–448. https://doi.org/10.1093/schbul/sbw099.
Manoliu, A., Riedl, V., Zherdin, A., Mühlau, M., Schwerthöffer, D., Scherr, M., Peters, H., Zimmer, C., Förstl, H., Bäuml, J., Wohlschläger, A.M., Sorg, C., 2013. Aberrant dependence of default mode/central executive network interactions on anterior insular salience network activity in schizophrenia. Schizophr. Bull. 40 (2), 428–437.
Mueller, F., Musso, F., London, M., de Boer, P., Zacharias, N., Winterer, G., 2018. Pharmacological fMRI: effects of subanesthetic ketamine on resting-state functional connectivity in the default mode network, salience network, dorsal attention network and executive control network. NeuroImage 19, 745–757. https://doi.org/10.1016/j.nicl.2018.05.037.
Nekovarova, T., Fajnerova, I., Horacek, J., Spaniel, F., 2014. Bridging disparate symptoms of schizophrenia: a triple network dysfunction theory. Front. Behav. Neurosci. 8, 171. https://doi.org/10.3389/fnbeh.2014.00171.
Pergola, G., Selvaggi, P., Trizio, S., Bertolino, A., Blasi, G., 2015. The role of the thalamus in schizophrenia from a neuroimaging perspective. Neurosci. Biobehav. Rev. 54, 57–75.
Pollak, T.A., De Simoni, S., Barimani, B., et al., 2015. Phenomenologically distinct psychotomimetic effects of ketamine are associated with cerebral, blood flow changes in functionally relevant cerebral foci: a continuous arterial spin labeling study. Psychopharmacology 232, 4515. https://doi.org/10.1007/s00213-015-4078-8.
Power, J.D., Cohen, A.L., Nelson, S.M., Wig, G.S., Barnes, K.A., Church, J.A., ... Petersen, S.E., 2011. Functional network organization of the human brain. Neuron 72 (4), 665–678. https://doi.org/10.1016/j.neuron.2011.09.006.
Powers III, A.R., Kelley, M., Corlett, P.R., 2016. Hallucinations as top-down effects on perception. Biol. Psychiatry Cogn. Neurosci. Neuroimaging 1 (5), 393–400. https://doi.org/10.1016/j.bpsc.2016.04.003.
Raichle, M.E., 2015. The brain's default mode network. Annu. Rev. Neurosci. 38, 433–447. https://doi.org/10.1146/annurev-neuro-071013-014030.
Raichle, M.E., MacLeod, A.M., Snyder, A.Z., Powers, W.J., Gusnard, D.A., Shulman, G.L., 2001. A default mode of brain function. Proc. Natl. Acad. Sci. U. S. A. 98 (2), 676–682. https://doi.org/10.1073/pnas.98.2.676.
Shaffer, C.L., Osgood, S.M., Smith, D.L., Liu, J., Trapa, P.E., 2014. Enhancing ketamine translational pharmacology via receptor occupancy normalization. Neuropharmacology 86, 174–180. https://doi.org/10.1016/j.neuropharm.2014.07.008.
Sheffield, J.M., Barch, D.M., 2016. Cognition and resting-state functional connectivity in schizophrenia. Neurosci. Biobehav. Rev. 61, 108–120. https://doi.org/10.1016/j.neubiorev.2015.12.007.
White, T.P., Joseph, V., Francis, S.T., Liddle, P.F., 2010. Aberrant salience network (bilateral insula and anterior cingulate cortex) connectivity during information processing in schizophrenia. Schizophr. Res. 123 (2–3), 105–115.
Whitfield-Gabrieli, S., Nieto-Castanon, A., 2012. Conn: a functional connectivity toolbox for correlated and anticorrelated brain networks. Brain Connect. 2 (3), 125–141. https://doi.org/10.1089/brain.2012.0073.
Whitfield-Gabrieli, S., Thermenos, H.W., Milanovic, S., Tsuang, M.T., Faraone, S.V., McCarley, R.W., ... Seidman, L.J., 2009. Hyperactivity and hyperconnectivity of the default network in schizophrenia and in first-degree relatives of persons with schizophrenia. Proc. Natl. Acad. Sci. U. S. A. 106 (4), 1279–1284. https://doi.org/10.1073/pnas.0809141106.
Wotruba, D., Michels, L., Buechler, R., Metzler, S., Theodoridou, A., Gerstenberg, M., ... Heekeren, K., 2014. Aberrant coupling within and across the default mode, task-positive, and salience network in subjects at risk for psychosis. Schizophr. Bull. 40 (5), 1095–1104. https://doi.org/10.1093/schbul/sbt161.
Zhou, Y., Zeidman, P., Wu, S., Razi, A., Chen, C., Yang, L., ... Friston, K.J., 2017. Altered intrinsic and extrinsic connectivity in schizophrenia. Neuroimage Clin. 17, 704–716. https://doi.org/10.1016/j.nicl.2017.12.006.
Zhou, Y., Friston, K.J., Zeidman, P., Chen, J., Li, S., Razi, A., 2018. The hierarchical organization of the default, dorsal attention and salience networks in adolescents and young adults. Cereb. Cortex 28 (2), 726–737. https://doi.org/10.1093/cercor/bhx307.